Journal of Catalysis 262 (2009) 150–158

Contents lists available at ScienceDirect

Journal of Catalysis

www.elsevier.com/locate/jcat

Influence of heterogenization on catalytic behavior of mono- and bimetallic nanoparticles formed in poly(styrene)-*block*-poly(4-vinylpyridine) micelles

Esther M. Sulman [a], Valentina G. Matveeva [a], Mikhail G. Sulman [b], Galina N. Demidenko [a], Pyotr M. Valetsky [b], Barry Stein [c], Tom Mates [d], Lyudmila M. Bronstein [e,*]

[a] *Tver Technical University, A. Nikitin St., 22, Tver 170026, Russia*
[b] *Nesmeyanov Institute of Organoelement Compounds, 28 Vavilov St., Moscow 119991, Russia*
[c] *Department of Biology, Indiana University, Bloomington, IN 47405, USA*
[d] *Materials Department, University of California, Santa Barbara, CA 93106, USA*
[e] *Department of Chemistry, Indiana University, Bloomington, IN 47405, USA*

ARTICLE INFO

Article history:
Received 1 August 2008
Revised 4 November 2008
Accepted 19 December 2008
Available online 21 January 2009

Keywords:
Catalysis
Nanoparticles
Block copolymer
Heterogenized

ABSTRACT

Influence of heterogenization on catalytic properties of block copolymer micellar catalysts derived from polystyrene-*block*-poly-4-vinylpyridine and containing Pd monometallic and bimetallic PdAu, PdPt, and PdZn nanoparticles has been studied in selective hydrogenation of the triple bond of 3,7-dimethyloctaen-6-yne-1-ol-3 (dehydrolinalool). We demonstrate that the heterogenization can both increase and decrease catalytic activity depending on the type of NPs. In the absence of a modifying metal (Pd monometallic nanoparticles) or for PdZn nanoparticles where Zn is the electron donor, the activity of heterogenized catalysts increases, while for PdAu and PdPt based catalysts, where the modifying metal is the electron acceptor, the activity decreases. These changes are explained by the increased polarity of the catalyst after deposition on alumina (addition of a component with a higher dielectric constant) offset by poor accessibility of some catalytic sites of nanoparticles containing electron deficient Pd atoms.

1. Introduction

The major aspiration of modern catalytic studies is development of catalysts possessing high selectivity (up to 100%), activity and stability along with robustness to make them technologically relevant. This goal can be achieved by designing supported catalysts containing very active catalytic species such as nanoparticles (NPs) [1]. Controlling the size, shape and surface distribution of catalytic nanoparticles, and also the type of support allows development of novel and efficient heterogeneous catalysts [2–7].

In the last decade catalysts based on nanoparticles formed in various types of nanostructured polymers were actively studied in a number of catalytic reactions [8–11]. The major advantages of nanostructured systems, such as block copolymer micelles, dendrimers, ultra-thin layers, etc. are the small sizes (in a nanometer range) of the nanoparticle-containing zones, eliminating internal diffusion limitations and providing good reactant accessibility to NPs. Catalytic NPs can be formed in functionalized micelle cores of block copolymer micelles and used in various catalytic reactions [12,13]. For example, Pd nanoparticles formed in the polystyrene-*block*-poly-4-vinylpyridine (PS-*b*-P4VP) micelles were used as a catalyst of cross-coupling reaction between aryl halides and alkenes [13]. In our earlier work the PS-*b*-P4VP micelles containing Pd and Pd/Au nanoparticles were studied in hydrogenation of cyclohexene, 1,3-cyclooctadiene, and 1,3-cyclohexadiene [12]. It was demonstrated that the synthetic pathway to form NPs and the type of reducing agent strongly influence the catalytic activity of NPs. The lowest activity was observed for $N_2H_4{\cdot}H_2O$ reduction which is related to a morphology where only a small number of noble metal colloids is embedded in the micelle core. The highest activity was obtained for the super-hydride reduction where the formation of many metal NPs per micelle is observed

Au nanoclusters formed in the PS-*b*-P2VP micelles were used in catalytic electrooxidation of CO [14,15]. Triblock and diblock copolymer based nanospheres were employed in hydrogenation of alkenes and methyl methacrylate [16,17]. Formation of NPs in the block copolymer coronas allows better access to the nanoparticle surface and high catalytic activity but stabilization of NPs is poor, leading to their aggregation [18,19].

The homogeneous catalysts based on NP-containing block copolymers were used to form heterogeneous catalysts. Amphiphilic polystyrene–poly(ethylene glycol) resin supported Pd nanoparticles exhibited high catalytic performance in hydrogenation of olefins and hydrodechlorination of chloroarenes under aqueous conditions [20].

* Corresponding author.
E-mail address: lybronst@indiana.edu (L.M. Bronstein).

0021-9517/$ – see front matter
doi:10.1016/j.jcat.2008.12.022

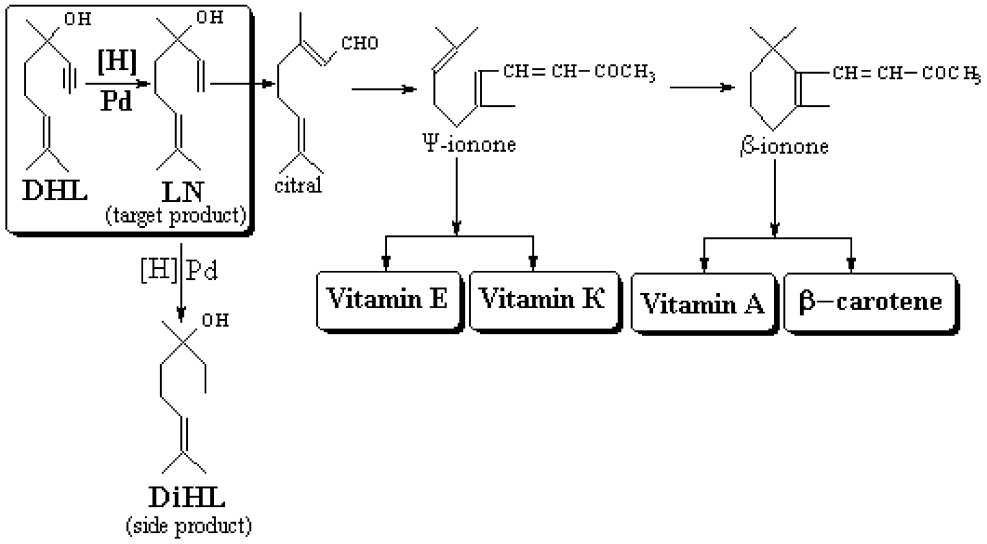

Scheme 1. The reaction path of the DHL hydrogenation and possible products of further transformations.

In our preceding paper [21] we reported catalytic properties of monometallic Pd and bimetallic PdAu, PdPt, and PdZn NPs formed in the cores of the PS-*b*-P4VP micelles in selective hydrogenation of dehydrolinalool (3,7-dimethyloctaen-6-yne-1-ol-3, DHL) to linalool (3,7-dimethyloctadiene-1,6-ol-3, LN). The presence of the second metal (metal-modifier) in a NP was found to influence the catalytic properties by modifying the structure and morphology of NPs. These catalysts displayed excellent selectivity (up to 99.8% at 100% conversion) and high activity, however the need of separation of such catalysts from the reaction medium for multiple uses makes them unsuitable for any commercial applications. The solution of this problem is heterogenization of micellar catalysts on inorganic supports which are traditionally used in heterogeneous catalysis. In this way the advantages of well-defined NPs formed in block copolymer micelles are combined with robustness of heterogeneous systems. We expected that the catalytic activity and selectivity of these catalysts should be comparable with their micellar precursors; however the influence of the support is difficult to predict. Each component in the catalytic system (NPs, polymer stabilizer, support) and their interaction can strongly influence the catalytic behavior [22–25]. To comprehend a catalytic process, the influence of each component should be understood. This can be done using reactivity studies, i.e., by exploring these catalysts in the catalytic reaction [3].

In this paper we report the structure and catalytic studies of the heterogenized (on alumina) micellar catalysts based on monometallic Pd and bimetallic PdAu, PdPt, and PdZn NPs formed in the PS-*b*-P4VP block copolymer micelles. As a catalytic reaction of interest, we chose DHL hydrogenation because it was thoroughly investigated by us earlier [4,21,26] and because the reaction product is a valuable substance: fragrance, antimicrobial and antifungal substance, and intermediate product of some vitamins (Scheme 1) [27–29]. Unlike well documented electronic effects, data on the influence of metal–support interaction on the activity of the supported catalysts are limited [30–32]. The influence of the support on metal may consist of several factors: (i) changing of a NP charge (if the support is conductive), (ii) influence on NP morphology (if NPs are formed directly on the support), and (iii) formation of new catalytic sites at the metal–support interface [33–35].

Here we demonstrate that the heterogenization does not influence NP morphology, but alters catalytic properties and these changes depend on a nanoparticle structure. The catalytic activity may both increase and decrease governed by the NP type.

2. Experimental

2.1. Materials

Diblock copolymer polystyrene-*block*-poly-4-vinylpyridine (PS-*b*-P4VP) $M_n = 19400$, $M_w = 22500$, $X_{4\text{-VP}}$ (relative 4-VP content) = 0.340, was prepared using living anionic polymerization (MPI of Colloids and Interfaces, Potsdam/Golm, Germany) as published elsewhere [36,37]. $HAuCl_4 \cdot 3H_2O$, $Pd(CH_3COO)_2$, $Zn(CH_3COO)_2$ $K[Pt(C_2H_4)Cl_3] \cdot H_2O$ (Zeise salt) $LiB(C_2H_5)_3H$ (super-hydride, 1 M solution of $LiB(C_2H_5)_3H$ in THF) were obtained from Aldrich and used as received. Toluene (Aldrich) was twice distilled under KOH. Petroleum ether (Fluka) was distilled under metallic sodium in the Ar counterflow. Other solvents were used as received. Al_2O_3 (Fluka, mesostructured, 60 μk, for chromatography) was annealed at 450 °C for 5 h. Pd/Al_2O_3 (0.5 wt% Pd) was obtained from Degussa AG.

2.2. Preparation of catalysts

Block copolymer micelles containing mono- and bimetallic nanoparticles (homogeneous micellar catalyst) were prepared according to the procedure published elsewhere [12,21,38]. In a typical experiment, PS-*b*-P4VP block copolymer was dissolved in toluene at concentration of 10 g/L under vigorous stirring for 1 h. The metal compounds were added to the polymer solutions under air and stirred for 24 h at room temperature (molar ratio N/Pd = 3/1, Pd/Au = 4/1, Pd/Pt = 4/1, Pd/Zn = 4/1, where N is the nitrogen of 4-VP units). For bimetallic systems, addition of both salts was carried out simultaneously. After 24 h stirring, the resulting metal-containing polymer solution was filtered from the unreacted metal compounds or insoluble by-products of the reaction (KCl in the case of Zeise salt) through a Millipore 0.45 μm PTFE filter. Reduction of Pd or bimetallic samples was performed in a two-neck flask equipped with a stopcock, rubber septum and a Teflon stir bar. Super-hydride was used in five-fold molar excess. In all the cases reduction was carried out under argon after a standard degassing procedure [12]. Airless transfer of solutions was achieved by Hamilton syringe techniques.

The heterogeneous catalysts were prepared by impregnation of 1 g of Al_2O_3 with 1 mL of a toluene solution of PS-*b*-P4VP micelles containing metal nanoparticles (3.5×10^{-3} mol Pd/L) for 10 min stirring (all solution was adsorbed) followed by drying in a vacuum oven at 50 °C. Note that 1 g of alumina used in this study

can absorb 2.5 mL of toluene so one might expect only surface deposition of block copolymer micelles on alumina. Metal contents in heterogeneous catalysts were obtained by X-ray fluorescent analysis as described below.

2.3. Measurements

X-ray photoelectron spectroscopy (XPS) scans were collected on a Kratos Axis Ultra spectrometer (Kratos Analytical, Manchester, UK). Monochromated Al K$\alpha_{1,2}$ 1486.6 eV radiation was used as an excitation source. Charge neutralization from a low-energy electron filament was used. The survey scans were run at 160 eV pass energy and 0.5 eV channel width, and the Pd high-resolution scans were run at 40 eV pass energy and a 0.1 eV channel width. All binding energies (BE) were referenced to aliphatic C 1s at 284.9 eV.

The BET specific surface area and pore size distribution of the support and the catalysts were determined using a Beckman Coulter^{TM} SA 3100^{TM} (Coulter Corporation, Miami, Florida) instrument via N_2 adsorption–desorption at 77 K.

Samples of micellar catalysts for transmission electron microscopy (TEM) were prepared by evaporation of 10^{-4} mol/L THF solutions under air. Electron micrographs of the samples were obtained with a Zeiss 912 Omega electron microscope. Heterogenized samples were placed in flat embedding molds with EMbed 812-Araldite 502 resin or Spurr's low viscosity resin and polymerized at 65 °C for 12 h. The polymerized blocks were cut using a Porter-Blum MT 2 ultramicrotome. Ultrathin sections were placed on 400 mesh copper grids. Grids were viewed with a JEOL 1010 TEM

Pd, Pt, Au, Zn and Al contents were determined using X-ray fluorescence analysis (XFA) performed with a Zeiss Jena VRA-30 spectrometer equipped with a Mo anode, a LiF crystal analyzer, and a SZ detector. Analyses were based on the corresponding K_α lines [39]. A series of standards were prepared by mixing 1 g of polystyrene with 10–20 mg of standard compounds. The time of data acquisition was held constant at 10 s.

2.4. DHL hydrogenation

The catalytic reaction was carried out by the method described elsewhere [21]. In a typical experiment, a glass batch isothermal reactor installed in a shaker (maximum 960 shakings per minute without diffusion limitations) has been used. The reactor was equipped with two inlets: for catalyst, solvent, and substrate loading and for hydrogen feeding. Before substrate has been charged into the reactor, catalyst was pretreated with H_2 for 60 min at 90 °C to saturate the NP surface with hydrogen due to adsorption [40]. DHL concentration (C_o), catalyst amount (C_c) and hydrogenation temperature (t_h) have been varied. The experiments were carried out at atmospheric pressure.

Analysis of reaction mixture has been performed by gas chromatography (GC) using chromatograph "CHROM-5" with FID and glass column 3 m/3 mm. The column has been filled with solid phase "Chromaton N" (0.16–0.20 mm) saturated with carbowax 20 M (10% of liquid phase to support weight).

For stability studies, the catalyst was separated from the reaction medium by filtration, washed with toluene five times and dried in vacuum at 100 °C.

3. Results and discussion

3.1. Morphology of the heterogeneous catalysts

In the preceding work [21,26] we studied the influence of a metal-modifier and a PS-*b*-P4VP block copolymer on nanoparticle formation and catalytic properties. The PS-*b*-P4VP micelles were found to play a dual role: they stabilize NPs and control the NP growth, while the 4-VP units modify the NP surface and provide high selectivity in hydrogenation of a triple bond to a double one [26]. The influence of a modifying metal (toward Pd) on NP morphology and catalytic properties was investigated using the FTIR studies of the CO adsorption and XPS [21]. The FTIR spectra of PdPt and PdZn NPs were found to display two bands in the region of terminal CO absorption, while Pd and PdAu samples exhibit only one band in this region. The lack of the second terminal band for CO adsorption for PdAu shows that there are no Au atoms on the particle surface. Therefore, we surmised that for PdAu bimetallics, core–shell structure forms, while for PdPt and PdZn NPs, cluster-in-cluster structures are obtained [21].

In this paper we interrogate the influence of heterogenization of the monometallic and bimetallic nanoparticles formed in PS-*b*-P4VP on catalytic properties of these systems. Heterogeneous catalysts were prepared by impregnation of inorganic support (alumina) with a precursor: a toluene solution of the NP-containing PS-*b*-P4VP block copolymer micelles. The NPs were formed in block copolymer micelles prior to heterogenization by incorporation of metal compounds followed by their reduction with a strong reducing agent: super-hydride [21]. It is noteworthy, that these catalytic systems are exceptionally complex: they consist of NPs (both mono- and bimetallic), block copolymer micelles surrounding NPs, and alumina support. Each component may influence the behavior of one or more other components, changing the NP or micelle morphology or exerting the electronic influence.

Fig. 1 shows TEM images of the micellar sample containing Pd–Au NPs (homogeneous catalyst) and of the heterogenized catalyst based on the same micellar precursor. In the TEM image of the micellar sample one can see the dark diffuse circles representing the PS-*b*-P4VP micelles and the darker small dots which are NPs. The mean NP diameter and standard deviation are 1.6 nm and 0.2 nm, respectively (calculated out of 200 NPs). In a number of areas of the image (where micelles do not overlap) one can see that the NPs are organized in a circular pattern surrounding the micelles (or cores) (see blue arrows, Fig. 1). This suggests that the NPs form at the core/corona interface. This seems to be reasonable because during reduction the reducing agent (super-hydride) slowly penetrates the P4VP micelle core which is in a quasi-solid state, thus nucleation starts from the micelle periphery. Unlike the micellar sample, in heterogenized catalyst (Fig. 1b) the high electron contrast of alumina obscures a clear view of NPs, although in the areas of lesser contrast the NPs can be distinguished as indicated by red arrows. The inset in Fig. 1b shows a higher magnification image for better viewing of NPs. The NP size and standard deviation are 1.5 nm and 0.2 nm, respectively (calculated out of 85 NPs). The TEM image in Fig. 1b also demonstrates that the block copolymer micelles do not exist between the alumina grains, suggesting that they are adsorbed on the alumina surface. Similar images were observed for other heterogenized catalysts.

Comparison of the TEM images before and after heterogenization reveals that the NP size and shape remain basically unchanged and the NPs do not aggregate. This suggests that NP morphology (core–shell or cluster-in-cluster) is preserved under heterogenization due to surrounding P4VP stabilizing NPs.

The elemental analysis data of the heterogenized catalysts carried out using X-ray fluorescence spectroscopy are presented in Table 1. These data demonstrate that for all the catalysts, C, N, and metal contents are very low, revealing that only a small fraction of PS-*b*-P4VP containing NPs (we assume a thin layer) is adsorbed on alumina. Indeed, comparison of these data with the XPS data presented in Table 2 shows enrichment of the surface layer with Pd, C, and N and a lower content of Al and O, revealing that the block copolymer and NPs are located in the surface layer of the catalysts. (Note that the XPS penetration depth in polymeric systems is $\leqslant$10 nm while it is much lower in metal oxides and metals

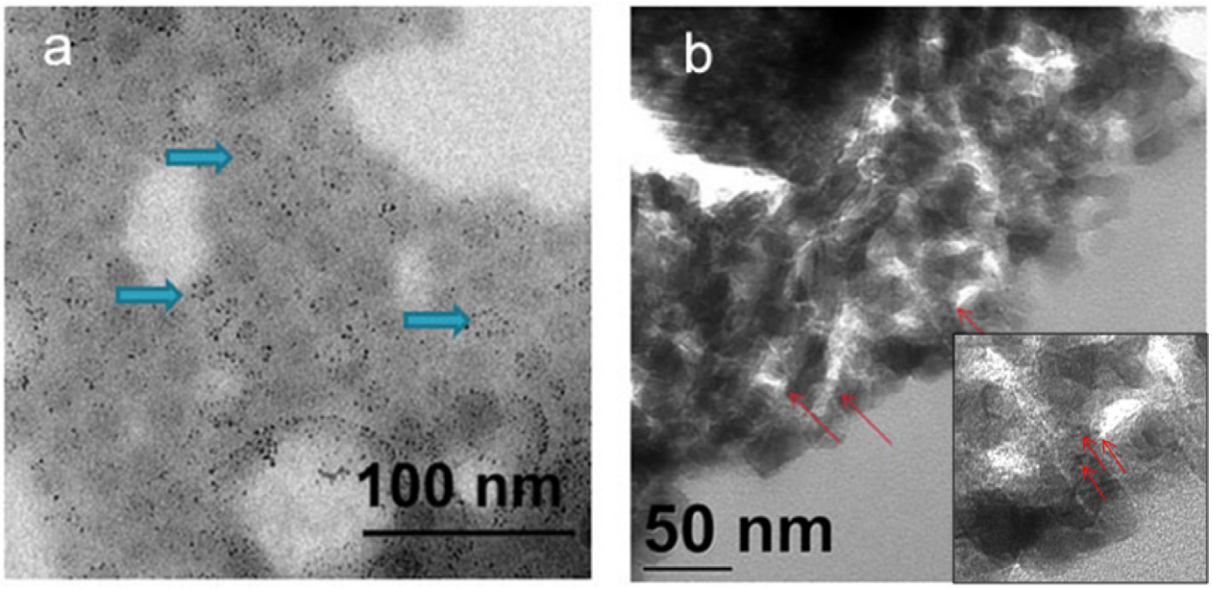

Fig. 1. TEM images of the PS-*b*-P4VP micelles containing PdAu NPs (a) and the cross-section of the heterogenized catalyst (b). Blue arrows in (a) show circular patterns of the NP arrangement in block copolymer micelles. Red arrows in (b) show NPs. The inset in (b) shows the higher magnification image. (For interpretation of the references to color in this figure legend, the reader is referred to the web version of this article.)

Table 1
The elemental analysis data of the heterogenized catalysts based on XFA.

Sample	Elemental analysis data, wt%					
	C	H	N	Al	Pd	Metal-modifier
PS-*b*-P4VP–Pd/Al_2O_3	0.94	0.09	0.07	48.5	0.02	–
PS-*b*-P4VP–PdAu/Al_2O_3	0.87	0.08	0.07	47.6	0.02	0.01
PS-*b*-P4VP–PdPt/Al_2O_3	1.05	0.13	0.10	42.7	0.03	0.02
PS-*b*-P4VP–PdZn/Al_2O_3	1.09	0.15	0.15	41.4	0.04	0.02

Table 3
The characteristics of the support and the heterogenized catalysts obtained from the nitrogen adsorption–desorption experiments.

Sample	S_{BET}, m^2/g	Pore volume, cm^3/g
Alumina	104.1	0.27
Pd/Al_2O_3	88.3	0.24
PS-*b*-P4VP–Pd/Al_2O_3	32.7	0.19
PS-*b*-P4VP–PdAu/Al_2O_3	34.5	0.14
PS-*b*-P4VP–PdPt/Al_2O_3	27.3	0.15
PS-*b*-P4VP–PdZn/Al_2O_3	39.9	0.18

[41,42].) For convenient comparison, Table 2 shows element contents both in atomic and weight percents.

The BET specific surface area and pore size distribution of the support and the heterogenized catalysts are presented in Table 3. The nitrogen adsorption–desorption experiments show a significant decrease of the surface area (approximately by a factor of three) after deposition of the block copolymer micelles on alumina, while the pore volume decreases only by 30–40%. This is consistent with the change in the pore size distribution (Fig. 2): the block copolymer micelles cover the alumina surface, filling all small (~4 nm) mesopores and about 70% of mesopores with a mean diameter of 8 nm, while the fraction of large mesopores (in the 12–30 nm range) slightly increases. We believe that the last event is due to intercalation of polymer into the smaller mesopores leading to their expansion [43,44]. On the contrary, for the Pd/Al_2O_3 catalyst, the pore volume and surface area decrease only by 10–20% indicating that the majority of the pores are not influenced by the Pd deposition in the absence of a polymer. The pore characteristics of the heterogenized micellar catalysts, however, are similar independently of the NP type, again suggesting that the changes observed in the support characteristics are due to block copolymer micelles.

3.2. Electronic structure of the catalysts

As was mentioned above, in our preceding work on micellar (homogeneous) mono- and bimetallic catalysts [21] the conclusion on the NP morphology (core–shell for PdAu vs cluster-in-cluster for PdPt and PdZn) were based on CO absorption. Such a study requires fairly high concentration of metal species. For the success of the FTIR experiments with micellar catalysts, the PS-*b*-P4VP solutions containing NPs, were concentrated before CO adsorption. In heterogenized catalysts, however, the metal content is low and similar studies cannot be done. Hence taking into account the integrity of the NPs during heterogenization of the micellar catalysts (from TEM), we conclude that their morphology (core–shell or cluster-in-cluster) stays unaltered as well.

The electronic effects in metal NP containing catalysts were studied using XPS. Depending on the nature of a metal-modifier (donor or acceptor of electrons toward Pd), it can make Pd more

Table 2
The elemental content in the heterogenized catalysts obtained from the XPS survey spectra.[a]

Sample	C, at%/C, wt%	N, at%/N, wt%	O, at%/O, wt%	Al, at%/Al, wt%	Pd, at%/Pd, wt%	Pt/Au/Zn, at%/Pt/Au/Zn, wt%
PS-*b*-P4VP–Pd/Al_2O_3	17.58/11.21	0.57/0.42	50.98/43.32	30.69/43.98	0.17/0.96	
PS-*b*-P4VP–PdAu/Al_2O_3	28.41/19.05	0.61/0.48	46.48/41.52	24.04/36.22	0.46/2.74	0.01/0.009
PS-*b*-P4VP–PdPt/Al_2O_3	17.80/11.55	0.48/0.36	52.88/45.36	28.61/41.38	0.24/1.35	–[b]
PS-*b*-P4VP–PdZn/Al_2O_3	19.46/12.95	0.33/0.24	52.49/45.60	27.55/40.36	0.13/0.75	0.03/0.01

[a] The method is not sensitive to hydrogen so the concentration of other elements is calculated without hydrogen content.
[b] The identification of Pt was not possible due to overlapping of Pt 4f and Al 2p levels while Pt 4d was not found due to weakness of the signal at low Pt content.

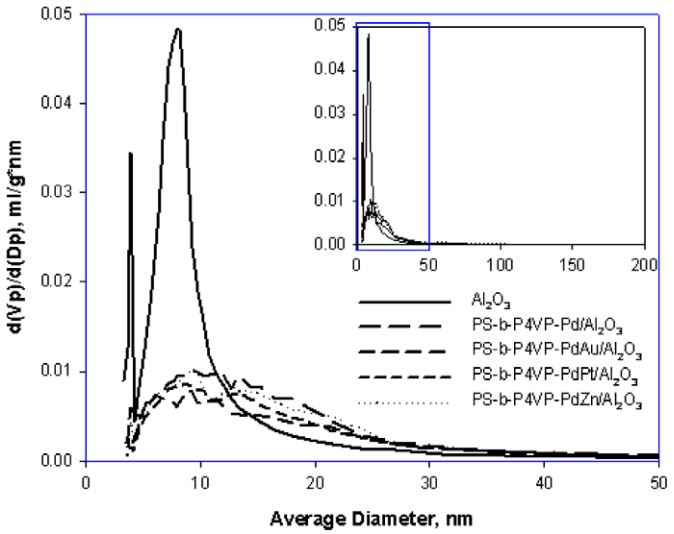

Fig. 2. Pore size distributions of alumina and the heterogenized catalysts.

Table 4
Pd $3d_{5/2}$ binding energies of the micellar homogeneous and heterogenized catalysts.

Compound	Pd $E_b3d_{5/2}$
Pd^0	335.7
$Pd(CH_3COO)_2$	339.0
PS-*b*-P4VP–Pd	335.1
PS-b-P4VP–Pd/Al_2O_3	**336.1, 338.1**
PS-*b*-P4VP–PdAu	335.5, 338.7
PS-b-P4VP–PdAu/Al_2O_3	**336.8, 339.0**
PS-*b*-P4VP–PdPt	335.6, 338.2
PS-b-P4VP–PdPt/Al_2O_3	–
PS-*b*-P4VP–PdZn	335.2, 337.1
PS-b-P4VP–PdZn/Al_2O_3	**335.8, 337.1**

electron-deficient (Au, Pt) or electron-rich (Zn) [45,46]. For the bimetallic PdAu, PdPt, and PdZn NPs in homogeneous micellar catalysts, the XPS data (Table 4) show a change of the binding energy of the fraction of Pd species toward higher oxidation state [21], while for Pd NPs, solely Pd^0 species were observed. Increase in binding energy could be attributed both to electronic effects in bimetallic samples and to charging the nanoparticles in nonconductive polymer environment (artifacts) which shows higher oxidation state than that of a real sample [47,48]. However, because this charging does not occur for Pd NPs but is noticeable for bimetallic ones (note that the samples were examined in identical conditions), this suggests the genuine influence of a modifying metal on the electronic structure of bimetallic colloids.

Upon heterogenization, the additional factor, such as support, appears which may influence the NP electronic properties [33,49,50]. Alumina may behave as a macroligand [51,52] toward the active metal leading to the electronic interaction of support and active metal which should determine stability of the reactant bonding in the reaction complex.

The example of the survey XPS spectrum is presented in Fig. 3 for Pd-containing heterogenized catalyst. The high resolution XPS Pd 3d spectra of heterogeneous catalysts are presented in Fig. 4, while Pd $3d_{5/2}$ binding energies of the micellar and heterogenized catalysts are shown in Table 4. Because in the PdPt sample, the Pd signal was rather weak and poorly resolved, the high resolution XPS spectra of three samples were compared: Pd, PdZn (donor influence) and Pd–Au (acceptor influence). Upon heterogenization of the Pd and PdAu micellar catalysts on alumina, the values of binding energies or the fraction of oxidized species increase (Fig. 4), suggesting a shift of the electron density toward more positively charged Pd atoms, which can be ascribed to the influence of the

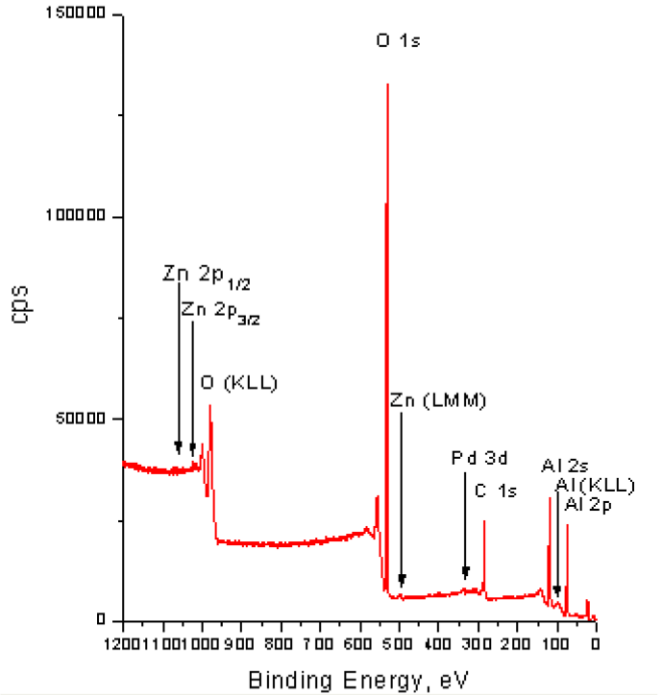

Fig. 3. Survey spectrum of the Pd heterogenized catalyst.

acceptor groups of alumina [53]. In the case of the Pd–Zn heterogenized catalyst, practically no shift of binding energy was observed because Zn is a strong donor and it counteracts the alumina influence. The binding energies of 338.1 and 337.1 eV for the Pd and PdZn heterogenized catalysts, respectively, can be assigned to the $Pd^{\delta+}$ species, while the binding energies of 336.1 and 335.8 eV, respectively, are assigned to Pd^0. The binding energy of 339.0 of the PdAu heterogenized catalyst should be assigned to Pd^{2+}, while that of 336.8 eV should be assigned to the $Pd^{\delta+}$ species.

The above changes assume that there should be close proximity between NPs and alumina to allow such influence. As was discussed above, the NPs are likely located at the micelle core/corona interface where the NP nucleation starts (Scheme 2). We believe that when the micelle deposition occurs, the polar micelle core (P4VP) adsorbs directly on alumina [54], while the hydrophobic PS chains tend to move away from the alumina surface. This should also lead to a micelle core deformation (toward disk-like cores) providing the maximum contact of the cores with the polar support. Such micelle deformation was described elsewhere [55] and should allow a direct contact of a number of NPs with alumina.

Thus, heterogenization of micellar catalysts on alumina is accompanied by a strong influence of the support on the electronic structure of Pd surface atoms. The whole heterogenized catalyst becomes more polar due to higher polarity of alumina than that of PS-*b*-P4VP. Indeed, the dielectric constant of alumina is 6–7 [56], while for PS-*b*-P4VP at room temperature, the dielectric constant was found to be in the range 3.2–3.8 (depending on a frequency). This suggests that the presence of alumina increases the dielectric constant of the whole heterogenized catalyst because the dielectric constant of a mixture is always higher than that of a less polar component. These changes may lead to a change of the catalytic properties of heterogenized micellar catalysts compared to homogeneous analogs as is discussed in the next section.

3.3. Kinetics of DHL hydrogenation

To understand the influence of heterogenization on selective DHL hydrogenation with micellar catalysts containing mono- and

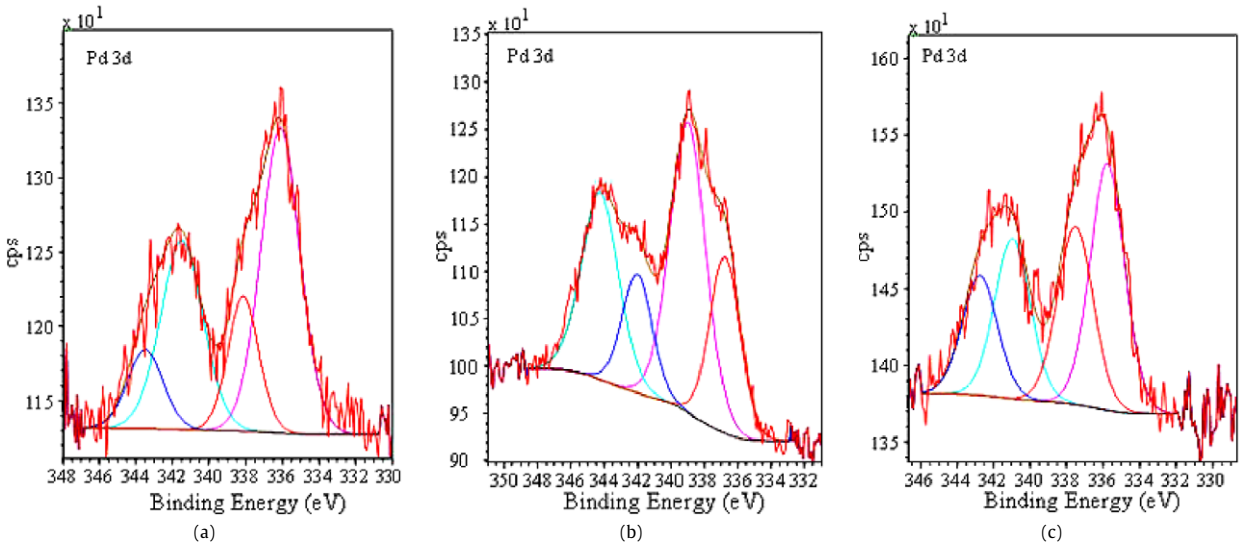

Fig. 4. High resolution XPS spectra of Pd (a), PdAu (b) and PdZn (c) heterogenized catalysts in the Pd $3d_{5/2}$ region.

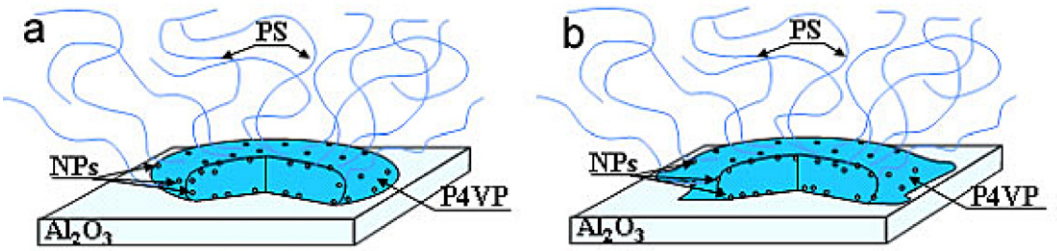

Scheme 2. Cartoons of adsorption of block copolymer micelles on alumina for Pd, PdZn (a) and PdAu, PdPt (b) nanoparticles. In (a) micellar core is only partially deformed due to adsorption on alumina while in (b) the micellar core spreads over alumina due to stronger adsorption.

bimetallic NPs, we studied the kinetics of the reaction. All experiments were carried out in toluene at a stirring rate of 960 shakings/min (without diffusion limitations) and varying concentrations of substrate and catalyst in the range of 0.22–0.88 mol/L (C_o) and 1.01×10^{-5}–4.08×10^{-5} mol of Pd/L (C_c), respectively, and varying a temperature in the range 50–95 °C. As a condition allowing evaluation of the dependence of DHL conversion on time at various C_0 and C_c values, we used the ratio $q = C_0/C_c$ (mol/mol) similar to our preceding work (Fig. 5) [21].

Based on the experimental data, we calculated the activity of the catalysts as moles of LN formed per second and per mole of Pd. The activity values are presented in Table 5 for both homogeneous and heterogenized micellar catalysts to reveal the influence of heterogenization.

To calculate the parameters of the Arrhenius equation, we varied the DHL hydrogenation temperature in the range 50–95 °C. From the Arrhenius dependence in the coordinates $\ln k - 1/T$, the pre-exponential factor k_0, which according to a number of reports is proportional to the amount of catalytic sites [57,58], and apparent activation energy E_a were calculated (Table 5).

$$k = k_0 \cdot e^{-E/RT}. \quad (1)$$

For the Pd monometallic catalyst, heterogenization has little effect on the activation energy but leads to nearly triple increase of a pre-exponential factor. This results in almost doubling of the catalyst activity (compare #1 and #2 in Table 5) [21,26]. We believe that when the micellar catalyst is deposited on alumina, the whole catalytic system becomes more polar (because the dielectric constant of alumina is higher than that of the block copolymer, see discussion in the previous section), creating more favorable conditions for the amphiphilic DHL molecules to access catalytic active sites. Indeed, in DHL the triple bond is located next to the OH group which should adsorb better on a polar catalyst (the higher the polarity of the adsorbent, the higher the polarity of the adsorbing species [59]). On the contrary, heterogenization of the PdAu based catalyst leads to a significant decrease in the pre-exponential factor (by four orders of magnitude) and therefore the amount of catalytic sites. At the same time, the activation energy for the PS-*b*-P4VP–PdAu/Al_2O_3 system also decreases compared to that of the homogeneous micellar catalyst. We think that the decrease of the activation energy is due to electron-withdrawing influence of the support (alumina [3,60,61]) on Pd atoms. This influence is especially noticeable for the core–shell structure of PdAu nanoparticles as these particles are mostly electron deficient due to the strong electron acceptor character of Au.

However, the significant decrease of the number of catalytic sites while all other conditions and components are identical is difficult to explain unless we assume the following: the adsorption on alumina of different structure NPs located on the core/corona interface is different. As was discussed above, adsorption of the PS-*b*-P4VP micelles on alumina should occur via the P4VP block (core), because the PS block is too hydrophobic (Scheme 2). We postulate that the monometallic Pd nanoparticles are moderately adsorbed on alumina, allowing free access of the reactant to all Pd surface atoms (Scheme 2a). As a result the presence of alumina only moderately increases the amount of catalytic sites (due to polarity increase, see discussion above) without a change of the activation energy. In the case of PdAu nanoparticles, where Au is an acceptor, we suggest that the adsorption of the PdAu nanoparticles located at the interface of the P4VP cores is much stronger, leading to decreased availability of Pd atoms as they are buried at the NP-core/alumina interface. Thus, the modification of the NP

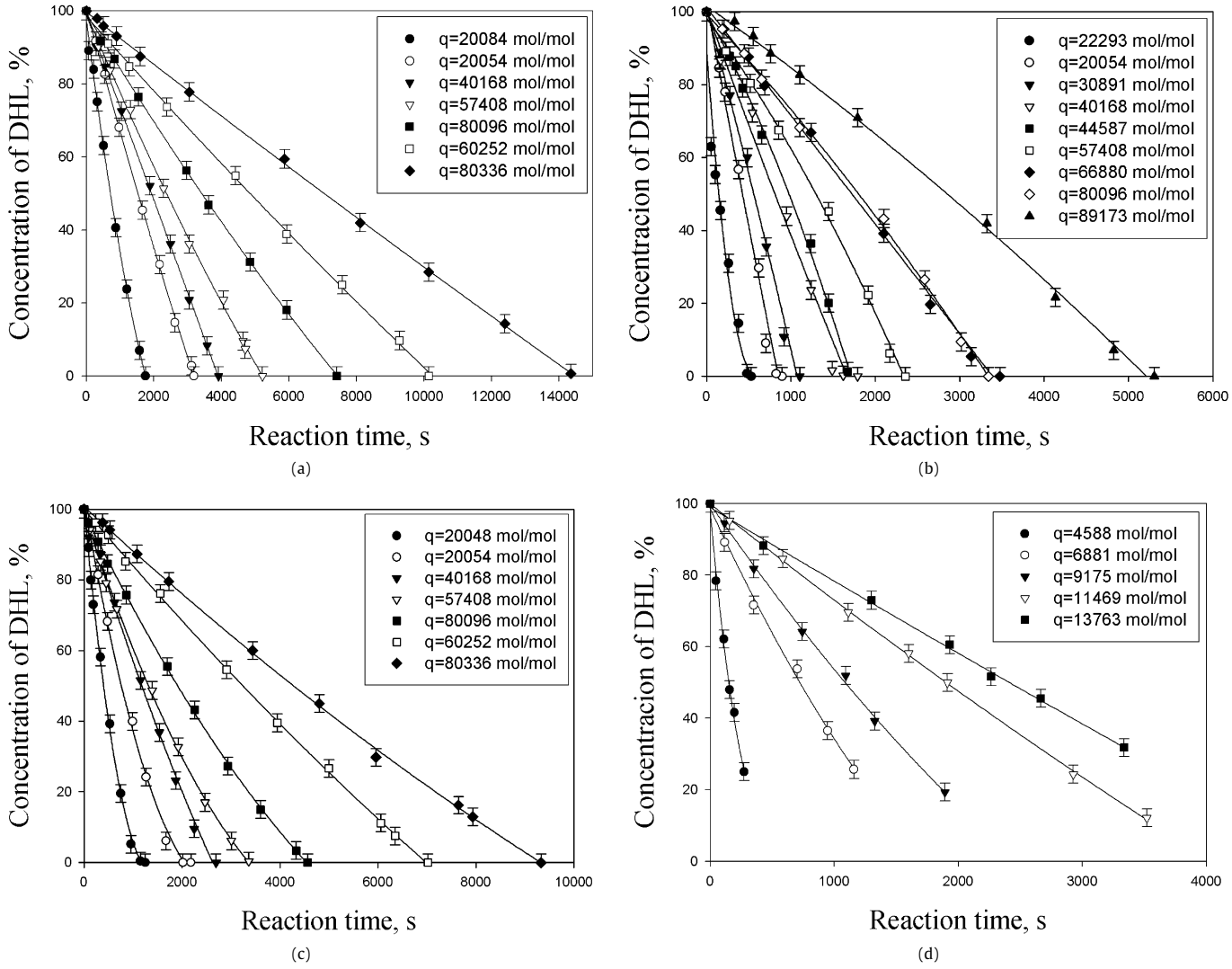

Fig. 5. Dependence of the DHL concentration on the reaction time with (a) PS-*b*-P4VP–Pd/Al_2O_3, (b) PS-*b*-P4VP–PdAu/Al_2O_3, (c) PS-*b*-P4VP–PdZn/Al_2O_3, (d) PS-*b*-P4VP–PdPt/Al_2O_3.

Table 5
Catalytic properties and kinetic parameters of the micellar homogeneous and heterogenized catalysts.[a]

#	Catalyst	Activity, mol LN mol Pd^{-1} s^{-1}	Selectivity,[b] %	E_a,[c] kJ/mol	k_0,[d] s^{-1}
1	PS-*b*-P4VP–Pd	18.5	99.0	23±4	66
2	PS-*b*-P4VP–Pd/Al_2O_3	58.3	98.0	27±4	190
3	PS-*b*-P4VP–PdAu	36.9	99.0	55±4	10^7
4	PS-*b*-P4VP–PdAu/Al_2O_3	27.3	98.0	30±4	1160
5	PS-*b*-P4VP–PdPt	49.2	98.5	26±4	659
6	PS-*b*-P4VP–PdPt/Al_2O_3	23.4	97.0	22±4	52
7	PS-*b*-P4VP–PdZn	34.4	98.5	26±4	356
8	PS-*b*-P4VP–PdZn/Al_2O_3	130.5	99.0	27±4	4226
9	Pd/Al_2O_3	0.76	88.0	56±4	9651

[a] Reaction conditions: 90 °C, 960 shaking/min (regime without diffusion limitations), toluene (30 mL), $C_o = 0.44$ mol/L, $C_c = 2.3 \times 10^{-5}$ mol Pd/L.
[b] This value is for 100% conversion.
[c] E_a is the activation energy.
[d] k_0 is the pre-exponential factor characterizing the amount of catalytic sites. The experimental error in k_0 determination is 5–7%.

properties due to alumina moderately decreases the activation energy but strongly decreases the amount of catalytic sites, leading overall to a decrease of the catalytic activity.

Similar results are obtained for the catalyst containing bimetallic PdPt NPs, where Pd is also coupled with an acceptor metal, but with weaker acceptor ability than that of Au. Here the amount of catalytic sites also decreases by one order of magnitude, while the activation energy is practically unaffected. Altogether it leads to a decrease of catalytic activity by a factor of two. For heterogenized PdZn based catalysts however, where Zn is a donor toward Pd, one might expect weaker adsorption of NP-containing cores on alumina (weaker than that of monometallic Pd based catalyst) leading to a significant increase in the amount of catalytic sites. Indeed we observe the k_0 increase (Table 5), while the activation energy does not change. Overall, this leads to the increase of the catalytic activity.

It is noteworthy to discuss another important feature of a catalytic reaction: an induction period. An induction period is the initial period of the reaction when complex reaction centers ("metal–support–substrate–solvent–hydrogen") are formed [62]. It may exist in all catalytic reactions but its length is different. If the induction period is too short, it is not observable. For the Pd and PdZn catalysts, the induction period was not observed (Fig. 5) revealing that the reaction sites already exist or are easily formed. For the PdAu catalyst, an induction period of 255 s is observed on the kinetic curve, revealing that the reactive catalytic complex is formed *in situ* during the hydrogenation. For PS-*b*-P4VP–PdPt/Al_2O_3, the induction period is also observed but it is much shorter: 160 s. We

Table 6
Catalytic properties of the heterogenized catalysts after repeated use.

Catalyst	Pd content, wt%		Selectivity, %		Activity, mol LN mol Pd^{-1} s^{-1}	
	Run 2[a]	Run 5	Run 2	Run 5	Run 2	Run 5
PS-*b*-P4VP–Pd/Al_2O_3	0.02	0.02	98.5	99.0	57.9	58.7
PS-*b*-P4VP–$PdAu/Al_2O_3$	0.02	0.02	99.0	98.0	27.0	27.2
PS-*b*-P4VP–$PdPt/Al_2O_3$	0.03	0.03	98.0	98.0	23.1	23.5
PS-*b*-P4VP–$PdZn/Al_2O_3$	0.04	0.04	98.5	99.0	128.3	131.4

[a] Run 1 is shown in Table 5.

believe that the stronger the acceptor properties of a modifier (toward Pd) leading to a stronger adsorption of NPs on alumina, the longer the induction period. Note that for the commercial Pd/Al_2O_3 where Pd is directly adsorbed on alumina, the induction period is 480 s [63].

Thus, for a donor modifying metal (or no modifying metal), deposition of block copolymer micelles on alumina results in the increase of the catalyst polarity (hydrophilization) and in better accessibility of catalytically active sites for an amphiphilic substrate (DHL). We believe that for acceptor modifying metals (Au and Pt), this phenomenon is offset by stronger adsorption of nanoparticles on alumina (Scheme 2b), leading to a decrease of the amount of available catalytic sites, hence leading to a decrease of catalytic activity.

We also studied stability of the heterogenized catalysts. All the catalysts demonstrated no activity or selectivity changes at the repeated use after five consecutive runs (Table 6). The elemental analysis data (Table 6) show no loss of active metal either, thus suggesting exceptional stability of the NPs formed in PS-*b*-P4VP and supported on alumina.

4. Conclusions

In this paper we demonstrated that deposition of NP containing micellar catalysts on alumina causes no changes in the NP morphology, but leads to different catalytic behavior depending on the NP structure. In the absence of the acceptor metal-modifier (for Pd and PdZn NPs), the key modifying factor is the increase of the polarity of the system upon heterogenization. This leads to the increase of the amount of catalytic sites and to the increase of the catalytic activity. When a metal-modifier is the acceptor (for PdAu and PdPt NPs), this leads to the electron deficiency of the surface Pd atoms and most likely their stronger adsorption on alumina, thus impeding access to some catalytic centers. This also results in the emergence of an induction period, the length of which is consistent with the acceptor ability of a modifying metal. Comparison of the catalysts studied in this work with the commercial Pd/Al_2O_3 shows that the activity of the heterogenized micellar catalysts containing mono- and bimetallic nanoparticles is much higher than that of the commercial catalyst owing to lower activation energy and/or higher amount of catalytic sites.

Acknowledgments

This work has been supported, in part, by the NATO Science for Peace Program (grant SfP-981438) and, in part, by Russian Foundation for Basic Research (grant 04-03-32928-a). We also thank Prof. Dr. M. Antonietti for the PS-*b*-P4VP sample and Dr. J. Hartmann for the TEM images of micellar samples.

References

[1] G.A. Somorjai, A.M. Contreras, M. Montano, R.M. Rioux, Proc. Natl. Acad. Sci. 103 (2006) 10577.
[2] C.R. Henry, Surf. Sci. Rep. 31 (1998) 231.
[3] H. Song, R.M. Rioux, J.D. Hoefelmeyer, R. Komor, K. Niesz, M. Grass, P. Yang, G.A. Somorjai, J. Am. Chem. Soc. 128 (2006) 3027.
[4] L.M. Bronstein, D.M. Chernyshov, R. Karlinsey, J.W. Zwanziger, V.G. Matveeva, E.M. Sulman, G.N. Demidenko, H.-P. Hentze, M. Antonietti, Chem. Mater. 15 (2003) 2623.
[5] P.L.L. Gunter, J.W. Niemantsverdriet, F.H. Ribeiro, G.A. Somorjai, Catal. Rev.-Sci. Eng. 39 (1997) 77.
[6] G.A. Somorjai, Y.G. Borodko, Catal. Lett. 76 (2001) 1.
[7] A.T. Bell, Science 299 (2003) 1688.
[8] D. Astruc, F. Lu, J.R. Aranzaes, Angew. Chem. Int. Ed. 44 (2005) 7852.
[9] C. Mueller, M.G. Nijkamp, D. Vogt, Eur. J. Inorg. Chem. 20 (2005) 4011.
[10] L.M. Bronstein, in: H.S. Nalwa (Ed.), Encyclopedia of Nanoscience and Nanotechnology, APS, Stevenson Ranch, CA, 2005, p. 193.
[11] N.V. Semagina, A.V. Bykov, E.M. Sulman, V.G. Matveeva, S.N. Sidorov, L.V. Dubrovina, P.M. Valetsky, O.I. Kiselyova, A.R. Khokhlov, B. Stein, L.M. Bronstein, J. Mol. Catal. A 208 (2004) 273.
[12] M.V. Seregina, L.M. Bronstein, O.A. Platonova, D.M. Chernyshov, P.M. Valetsky, J. Hartmann, E. Wenz, M. Antonietti, Chem. Mater. 9 (1997) 923.
[13] S. Klingelhoefer, W. Heitz, A. Greiner, S. Oestreich, S. Förster, M. Antonietti, J. Am. Chem. Soc. 119 (1997) 10116.
[14] T.F. Jaramillo, S.-H. Baeck, B.R. Cuenya, E.W. McFarland, J. Am. Chem. Soc. 125 (2003) 7148.
[15] B. Roldan Cuenya, S.-H. Baeck, T.F. Jaramillo, E.W. McFarland, J. Am. Chem. Soc. 125 (2003) 12928.
[16] R.S. Underhill, G. Liu, Chem. Mater. 12 (2000) 2082.
[17] Z. Lu, G. Liu, H. Phillips, J.M. Hill, J. Chang, R.A. Kydd, Nano Lett. 1 (2001) 683.
[18] A.B.R. Mayer, J.E. Mark, R.E. Morris, Polym. J. 30 (1998) 197.
[19] A.B.R. Mayer, J.E. Mark, Colloid Polym. Sci. 275 (1997) 333.
[20] R. Nakao, H. Rhee, Y. Uozumi, Org. Lett. 7 (2005) 163.
[21] L.M. Bronstein, D.M. Chernyshov, I.O. Volkov, M.G. Ezernitskaya, P.M. Valetsky, V.G. Matveeva, E.M. Sulman, J. Catal. 196 (2000) 302.
[22] J. Grunes, J. Zhu, G.A. Somorjai, Chem. Commun. 18 (2003) 2257.
[23] M. Boudart, J. Mol. Catal. 30 (1985) 27.
[24] D.R. Rolison, Science 299 (2003) 1698.
[25] K. Hayek, R. Kramer, Z. Paal, Appl. Catal. 162 (1997) 1.
[26] E. Sulman, Y. Bodrova, V. Matveeva, N. Semagina, L. Cerveny, V. Kurtc, L. Bronstein, O. Platonova, P. Valetsky, Appl. Catal. A 176 (1999) 75.
[27] A. Molnar, A. Sarkany, M. Varga, J. Mol. Catal. A Chem. 173 (2001) 185.
[28] V.V. Rusak, M.I. Zaretskii, A.S. Mozzhukhin, I.V. Usyshkina, L.A. Pushkina, Russ. J. Appl. Chem. 67 (1994) 1066.
[29] S. Pattnaik, V.R. Subramanyam, M. Bapaji, C.R. Kole, Microbios 89 (1997) 39.
[30] S.J. Tauster, S.C. Fung, R.L. Garten, J. Am. Chem. Soc. 100 (1978) 170.
[31] D.C. Koningsberger, J.H.A. Martens, R. Prins, D.R. Short, D.E. Sayers, J. Phys. Chem. 90 (1986) 3047.
[32] J.H.A. Martens, R. Prins, D.C. Koningsberger, Catal. Lett. 2 (1989) 211.
[33] P. Kacer, L. Cerveny, Appl. Catal. 229 (2002) 193.
[34] J. Barrault, A. Chafik, P. Gallezot, Appl. Catal. 67 (1991) 257.
[35] P. Ferreira-Aparicio, M. Fernandez-Garcia, A. Guerrero-Ruiz, I. Rodriguez-Ramos, J. Catal. 190 (2000) 296.
[36] M. Antonietti, J. Conrad, A. Thuenemann, Macromolecules 27 (1994) 6007.
[37] M. Antonietti, S. Foerster, S. Oestreich, J. Hartmann, E. Wenz, Nachr. Chem. Lab. Tech. 44 (1996) 579.
[38] M. Antonietti, E. Wenz, L. Bronstein, M. Seregina, Adv. Mater. 7 (1995) 1000.
[39] L.M. Bronstein, E.S. Mirzoeva, P.M. Valetsky, S.P. Solodovnikov, R.A. Register, J. Mater. Chem. 5 (1995) 1197.
[40] T. Mallat, Z. Bodnar, B. Minder, K. Borszeky, A. Baiker, J. Catal. 168 (1997) 183.
[41] D.R. Miller, N.A. Peppas, Macromolecules 20 (1987) 1257.
[42] Y.G. Li, Y.M. Lee, J.F. Porter, J. Mater. Sci. 37 (2002) 1959.
[43] E. Brunet, M.J. de la Mata, O. Juanes, J.C. Rodriguez-Ubis, Angew. Chem. Int. Ed. 43 (2004) 619.
[44] I.B. Tsvetkova, L.M. Bronstein, S.N. Sidorov, O.L. Lependina, M.G. Sulman, P.M. Valetsky, B. Stein, L.Z. Nikoshvili, V.G. Matveeva, A.I. Sidorov, B.B. Tikhonov, G.N. Demidenko, L. Kiwi-Minsker, E.M. Sulman, J. Mol. Catal. A Chem. 276 (2007) 116.
[45] A.J. Bard (Ed.), Encyclopedia of Electrochemistry of Elements, Dekker, New York/Basel, 1976.
[46] J.R. Bowser, Inorganic Chemistry, Brooks-Cole Publishing Co., Pacific Grove, CA, 1993, p. 805.
[47] C. Wagner, W. Riggs, L. Davis, G. Mullenberg, Handbook of X-Ray Photoelectron Spectroscopy, Perkin-Elmer Corporation, Minnesota, 1978.
[48] B.J. Tielsch, J.E. Fulghum, Surf. Interface Anal. 24 (1996) 422.
[49] B.H. Davis, in: G. Ertl, H. Knozinger, J. Weitkamp (Eds.), Handbook of Heterogeneous Catalysis, VCH, Weinheim, 1997, p. 13.
[50] J.M. Thomas, W.J. Thomas, Introduction to the Principles of Heterogeneous Catalysis, Academic Press, New York, 1967, p. 544.
[51] P. Gallezot, in: G. Ertl, H. Knozinger, J. Weitkamp (Eds.), Handbook of Heterogeneous Catalysis, VCH, Weinheim, 1997, p. 2209.
[52] B. Delmon, in: G. Ertl, H. Knozinger, J. Weitkamp (Eds.), Handbook of Heterogeneous Catalysis, VCH, Weinheim, 1997, p. 264.
[53] J.R. Anderson, Structure of Metallic Catalysts, Academic Press, London/New York/San Francisco, 1975, p. 462.

[54] K. Albrecht, A. Mourran, M. Moeller, Adv. Polym. Sci. 200 (2006) 57.
[55] M. Regenbrecht, S. Akari, S. Foerster, H. Mohwald, Surf. Interface Anal. 27 (1999) 418.
[56] W. Zhou, S. Qi, C. Tu, H. Zhao, C. Wang, J. Kou, J. Appl. Polym. Sci. 104 (2007) 1312.
[57] J. Gimenez, S. Cervera-March, Appl. Catal. 48 (1989) 307.
[58] M.M. Pakulska, C.M. Grgicak, J.B. Giorgi, Appl. Catal. A 332 (2007) 124.
[59] P.C. Hiemenz, R. Rajagopalan, Principles of Colloid and Surface Chemistry, 1997.
[60] R. Meyer, M. Baumer, S.K. Shaikhutdinov, H.-J. Freund, Surf. Sci. 546 (2003) 813.
[61] S.J. Tauster, S.C. Fung, J. Catal. 55 (1978) 29.
[62] M. Agnelli, H.M. Swaan, C. Marquezalvarez, G.A. Martin, C. Mirodatos, J. Catal. 175 (1998) 117.
[63] V.G. Matveeva, E.M. Sulman, T.V. Ankudnova, Kinet. Catal. 35 (1994) 385.